Available online at www.sciencedirect.com
SCIENCE DIRECT
Journal of Magnetic Resonance 178 (2006) 325–328
JMR Journal of Magnetic Resonance
www.elsevier.com/locate/jmr

Communication

Three dimensional magnetic resonance imaging by magnetic resonance force microscopy with a sharp magnetic needle

S. Tsuji [a,*], Y. Yoshinari [a], H.S. Park [b], D. Shindo [b]

[a] *Advanced Technology Division, JEOL Ltd., 3-1-2 Musashino, Akishima, Tokyo 196-8558, Japan*
[b] *Institute of Multidisciplinary Research for Advanced Materials, Tohoku University, Sendai 980-8577, Japan*

Received 16 June 2005; revised 5 October 2005
Available online 26 October 2005

Abstract

An electropolished magnetic needle made of $Nd_2Fe_{14}B$ permanent magnet was used for obtaining better spatial resolution than that achieved in our previous work. We observed the magnetic field gradient $|G_Z| = 80.0$ G/μm and the field strength $B = 1250$ G at $Z \sim 8.8$ μm from the top of the needle. The use of this needle for three dimensional magnetic resonance force microscopy at room temperature allowed us to achieve the voxel resolution to be 0.6 μm × 0.6 μm × 0.7 μm in the reconstructed image of DPPH phantom. The acquisition time spent for the whole data collection over 64 × 64 × 16 points, including an iterative signal average by six times per point, was about 10 days.

Keywords: MRFM; ESR; ESR imaging; Permanent magnet; Magnetic needle

Magnetic resonance force microscopy (MRFM) proposed by Sidles [1] is scanning probe microscopy combined with the magnetic resonance (MR) imaging technology. A few groups have already reported successful reconstruction of MRFM images [2–6], and their achieved spatial resolution and sensitivity were confirmed better than those of the conventional MR imaging. The incredible sensitivity have recently been proved by detecting single electron spin [7]. A small magnetic tip is essential in MRFM to generate a magnetic field gradient, which is a fundamental source to induce a force through the magnetic interaction with spins present in a sensitive slice where the magnetic resonance condition is satisfied. The modulated sample magnetization in the slice by the MR technique causes an oscillating force, which then excites an oscillation of a micrometer scale beam, so-called cantilever, typically used for atomic force microscopy. It is known that the smaller and shaper magnetic tip can generate the stronger magnetic field gradient, which makes the slice width narrower, resulting in a higher spatial resolution.

To improve our previously achieved resolution (~1 μm) [6], we used an electropolished magnetic needle made of a sintered $Nd_2Fe_{14}B$ permanent magnet [8,9]. The diameter of the most sharpened top was approximately 8 μm and gradually increased along the needle in 1 mm to reach the original rod diameter of 0.5 mm. The direction of magnetization was parallel to the symmetrical axis of the needle. Coercivity, remanence, and maximum-energy product of the magnetic needle were estimated to be 14.1 kOe, 13,900 G, and 368 kJ/m^3, respectively. This magnetic needle was then mounted on a three dimensional piezoelectric scanner installed in our MRFM spectrometer.

Knowledge of the magnetic field distribution in the very vicinity of the magnetic needle is crucial for MRFM imaging, especially when a point spread function is defined in the deconvolution, which comes in reconstructing the real image from the observed raw data. Thus, we first conducted examination of the field distribution by employing ESR–MRFM for a 5 μm diphenylpicrylhydrazil (DPPH) particle glued on a commercial cantilever (MikroMasch

* Corresponding author. Fax: +81 42 546 7225.
E-mail address: stsuji@jeol.co.jp (S. Tsuji).
URL: www.jeol.com (S. Tsuji).

1090-7807/$ - see front matter © 2005 Elsevier Inc. All rights reserved.
doi:10.1016/j.jmr.2005.10.002

CSC12). The microwave frequency $f = 2.0$–3.5 GHz, corresponding to the magnetic resonance field $B_0 = 714$–1250 G, was varied to characterize the overall field distribution. The measurements were carried out at room temperature and in vacuum of $\sim 10^{-3}$ Pa. The details of our MRFM spectrometer [6] and the procedure to map the magnetic field were described elsewhere [2–6].

The curved surface of constant B_0 specified by the given f was well fitted by the parabolic and axially symmetric formula [2]

$$B = B_0 + G_Z(Z - Z_0) + \frac{1}{2}G_{rr}r^2. \quad (1)$$

Here, the position (r,Z) is defined in the cylindrical coordinate where the Z axis coincides with the symmetrical axis of the magnetic needle. Z_0 is a distance between the top of the needle and the apex of the paraboloid. Importantly, this quantity is equivalent to a maximum depth for sensing the presence of spins below the sample surface. G_Z and G_{rr} are magnetic field gradients defined by $\partial B/\partial Z$ and $\partial^2 B/\partial r^2$, respectively. The radius of curvature R at the apex of the paraboloid is given approximately by $R = G_Z/G_{rr}$. Table 1 summarizes the values which were obtained in the series of these field mapping experiments. The strong magnetic field gradient exceeding $|G_Z| = 80.0$ G/μm and the high magnetic field strength of 1250 G were found at $Z \sim 8.8$ μm from the top of the needle.

Three dimensional (3D) ESR–MRFM imaging experiment was then carried out with this characterized magnetic needle. Fig. 1 shows the SEM (JSM-6060LA) image of a phantom used for verification of the imaging experiment, where two 5 μm DPPH particles glued on the cantilever were seen. Given at $f = 2.8$ GHz ($B_0 = 999.6$ G), the MR force map was three-dimensionally constructed in 40 μm × 40 μm × 11 μm volume meshed into $64 \times 64 \times 16$ points. The total acquisition time to complete the mapping, including an iterative average by six times per point, was about 10 days. Yet, we emphasize that our MRFM spectrometer is very stable and well regulated allowing to continue a long acquisition over weeks even at room temperature. The obtained force map was further processed for reconstructing the 3D real image through Wigner filtering deconvolution technique [2,3]. To define the point spread function, three parameters of the curved surface at constant magnetic field $B = B_0$ was determined by Eq. (1), and $Z_0 = 15.4$ μm,

Table 1
Property of the magnetic needle

Z_0 (μm)	B_0 (G)	G_z (G/μm)	G_{rr} (G/μm^2)	R (μm)
8.8	1250	−80.0	—	—
10.8	1142	−38.1	−3.01	12.7
18.2	928	−27.5	−1.12	24.7
30.4	714	−13.9	−0.292	47.7

Z_0 is a distance between the top of the magnetic tip and the apex of the paraboloid approximating the curved surface of constant magnetic field B_0 (see the text). G_Z and G_{rr} are the magnetic field gradient $\partial B/\partial Z$ and $\partial^2 B/\partial r^2$, respectively. R is a radius of curvature at the apex of the surface of constant B_0.

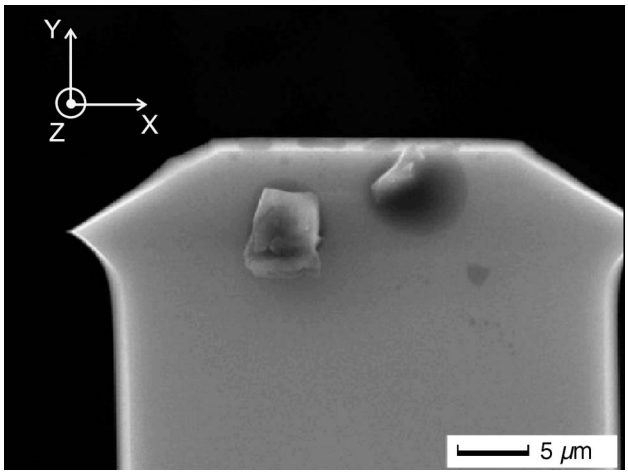

Fig. 1. SEM image of two DPPH particles glued on a cantilever.

$G_Z = -28.7$ G/μm, and $G_{rr} = -1.38$ G/μm^2 were finally derived.

Fig. 2A shows one of the Z slices of the reconstructed 3D-ESR image. The color grade indicates the number of spins per voxel of 0.625 μm × 0.625 μm × 0.688 μm. The maximum number of spins was 8.3×10^8 per voxel, or equivalently the spin density of 3×10^{21} spins/cm^3. The noise level was 1×10^8 per voxel, yielding a signal-to-noise ratio of ~8. The successive XY images sliced at different depths Z are also displayed in Fig. 2B, where a partial region of 25.63 μm × 13.75 μm × 3.44 μm around the objects is selectively chosen. Fig. 2C shows line profiles of the number of spins along the $X(Y)$ axis indicated by the horizontal(vertical) line in Fig. 2A, and along the Z axis on the crossed position of the two lines. The spatial resolution was defined as the width that the signal intensity decreased from 75 to 25% of its maximum on the edge of the spectral object [3]. By this definition, the resolutions were concluded to be 0.7 μm along the Z direction and 0.6 μm in the XY plane. The higher resolution than that previously reported in [6] was due to the larger magnetic field gradient produced by the sharp magnetic needle. The theoretical resolutions, which are determined by the magnetic field gradient and ESR linewidth of DPPH (~1 G) [2], are estimated to be 0.04 μm along the Z direction and 0.1 μm in the XY plane. The resolutions obtained in this experiment were limited by the scan step, not by the magnetic field gradient. Although the above theoretical resolution could be realized by mapping the force distribution with finer step, the sensitivity achieved in the present setup was insufficient to detect the signal from such a tiny voxel. One of the way to improve the sensitivity and the resolution is to operate MRFM in low temperature environment.

When the MRFM image shown in Fig. 2C is compared with the SEM image in Fig. 1, the number of DPPH particles, their relative positions and the size of the left particle were in reasonable agreement. On the other hand, the same comparison with respect to the shape and the size for the right particle is less satisfactory. One of the plausible

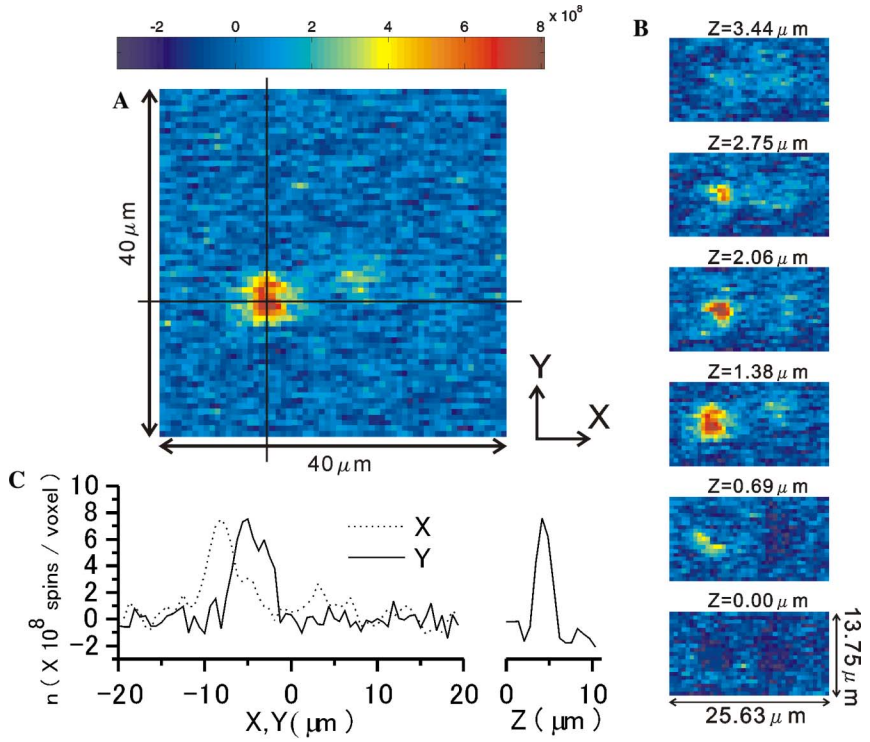

Fig. 2. 3D-ESR–MRFM images. (A) 2D XY image sliced at $Z = 1.38$ μm. The color grade indicates the number of spins present in each voxel. (B) Successive XY images sliced at different depths Z. (C) Line profiles of the number of spins along the $X(Y)$ axis indicated by the horizontal (vertical) line in (A), and along the Z axis on the crossed position of the two lines.

reasons for this inconsistency is that free radicals in the DPPH particles might become unstable to a possible chemical reaction with the glue. In addition, our empirical knowledge is that, the signal from DPPH particle always diminishes after exposition to the air over two to three months likely due to oxidation gradually invaded from the surface. If such damaged particle was accidentally chosen in the preparation, we could observe a weaker signal intensity. Finally, it should be noted that dark blue domains observed in the sliced images of $Z = 0.00$ and 0.69 μm in Fig. 2B implies the spin density to be negative. This falsely derived result is most likely due to a deviation of the approximated B_0 contour expressed by Eq. (1) from its true distribution, which causes an incomplete definition of the point spread function used in the delicate deconvolution process.

In summary, we used the electropolished sharp magnetic needle to improve the special resolution of MRFM. Through the examination of the local magnetic field distribution near the top of the needle by using MRFM, the field gradient $|G_Z| = 80.0$ G/μm and the magnetic field $B = 1250$ G were observed at $Z \sim 8.8$ μm from top of the needle. The 3D ESR–MRFM imaging experiment with this needle was carried out at room temperature for the phantom of 5 μm DPPH particles. The achieved resolution in the reconstructed MRFM image was 0.6 μm × 0.6 μm × 0.7 μm. The iterative averaging over 10 days was necessary to increase the signal-to-noise ratio up to ~8 in the reconstructed image. We however note that no group has so far achieved this resolution together with the stability in the room temperature MRFM imaging (Chao et al. [5] reported 3D imaging for DPPH with ~0.1 μm resolution yet at $T = 80$ K). Further improvements are under way.

Acknowledgment

We thank Y. Suzuki and K. Nagai for their help on the electron microscope measurements.

References

[1] J.A. Sidles, Folded Stern–Gerlach experiment as means for detecting nuclear magnetic resonance in individual nuclei, Phys. Rev. Lett. 68 (1992) 1124–1127.
[2] O. Zügar, D. Rugar, Magnetic resonance detection and imaging using force microscopy techniques, J. Appl. Phys. 75 (1994) 6211–6216.
[3] O. Zügar, S.T. Hoen, C.S. Yannoni, D. Rugar, Three-dimensional imaging with a nuclear magnetic resonance force microscope, J. Appl. Phys. 79 (1996) 1881–1884.
[4] K. Wago, D. Botkin, C.S. Yannoni, D. Rugar, Paramagnetic and ferromagnetic resonance imaging with a tip-on-cantilever magnetic resonance force microscope, Appl. Phys. Lett. 72 (1998) 2757–2759.
[5] S. Chao, W.M. Dougherty, J.L. Garbini, J.A. Sidles, Nanometer-scale magnetic resonance imaging, Rev. Sci. Instrum. 75 (2004) 1124–1127.
[6] S. Tsuji, T. Masumizu, Y. Yoshinari, Magnetic resonance imaging of isolated single liposome by magnetic resonance force microscopy, J. Magn. Reson. 167 (2004) 211–220.
[7] D. Rugar, R. Budakian, H.J. Mamin, B.W. Chui, Single spin detection by magnetic resonance force microscopy, Nature 430 (2004) 329–332.

[8] D. Shindo, Y.G. Park, Y. Gao, H.S. Park, Electron holography of Fe-based nanocrystalline magnetic materials, J. Appl. Phys. 95 (2004) 6521–6526.

[9] H.S. Park, Y.G. Park, Y. Gao, D. Shindo, M. Inoue, Direct observation of magnetization reversal in thin $Nd_2Fe_{14}B$ film, J. Appl. Phys. 97 (2005) 033908-1-4.